J Mater Sci (2009) 44:4407–4412
DOI 10.1007/s10853-009-3667-5

Synthesis of Fe_3O_4 polyhedra by hydrothermal method: using L-arginine as precipitator

Lianfeng Duan · Shusheng Jia · Yanjun Wang · Jian Chen · Lijun Zhao

Received: 18 March 2009 / Accepted: 4 June 2009 / Published online: 20 June 2009

Abstract Unusual polyhedral structures of cubic Fe_3O_4 were fabricated in high yield via a facile hydrothermal method in the presence of a surfactant cetyltrimethyammonium bromide (CTAB). Hexagonal, dodecahedral, truncated octahedral, and octahedral shapes can be prepared by changing the concentration of the CTAB in L-arginine solutions. In the solution-phase synthesis, both the L-arginine and CTAB were found to be the prime factors for the formation of the polyhedral structures. In addition, room-temperature vibrating sample magnetometer (VSM) testing results indicated that the magnetite synthesized without the addition of CTAB had the highest M_s value and the lowest H_c value. This synthesis method is also suitable for the preparation of other ferrites with spinel structure.

Introduction

The synthesis of architectural crystals has been the important research topics among materials science, because the properties of crystals depend not only on their composition but also on their structure, phase, shape, size, and size distribution [1–4].

The synthesis of magnetic particles has been intensively pursued because of their broad applications, including magnetic storage media, ferrofluids, magnetic resonance imaging, and magnetically guided drug delivery [5–8]. However, it is still a challenge to develop simple and reliable synthetic methods for the synthesis of magnetic materials with designed chemical components and controlled morphologies, which strongly affect the properties of magnetic materials. Now, numerous and diverse methodologies exist for building structures of many compositions and shapes on the magnetic materials while wet chemical techniques are still extensively used. These methods are being used to create isotropic particles as well as novel anisotropic structures, such as spheres [9], octahedra [10–12], rods [13], fractals [14], hollow structures [15], and nanosheets [16]. Whereas, there have been rare reports about the fabrication of Fe_3O_4 polyhedra.

Herein, a facile hydrothermal process is developed to synthesize Fe_3O_4 polyhedra. L-arginine and CTAB are used as precipitator and capping agent, respectively. Experimental results show that the L-arginine as the precipitator may be responsible for the formation of hexagonal Fe_3O_4 crystals. Furthermore, the influence of the CTAB on the morphologies of Fe_3O_4 crystals has been carefully investigated.

Experimental

Synthesis of magnetite

All chemicals used in this experiment were analytical grade and used without further purification. A total of 0.2 g of $Fe(SO_4)_2 \cdot 6H_2O$ and a certain amount of cetyltrimethyammoniumbromide (CTAB) were dissolved in 50 mL of distilled water to form a homogeneous solution with the N_2 flow. Next, 10 mL of L-arginine (0.2 mol L^{-1})

L. Duan · S. Jia · J. Chen · L. Zhao (✉)
Key Laboratory of Automobile Materials, Ministry of Education and Department of Materials Science and Engineering, Jilin University, Changchun 130022, People's Republic of China
e-mail: lijunzhao@jlu.edu.cn

Y. Wang
The Second Hospital of Jilin University, Changchun 130041, People's Republic of China

was added into the solution quickly at the room temperature with intensive stirring (30 min), which was then transferred into a 50 mL of Teflon-lined stainless steel autoclave, sealed and maintained at 180 °C for 24 h. After the reaction completed, the black-colored solid products were collected by magnetic filtration,and washed several times with distilled water and ethanol. The final products were dried in a vacuum oven at 40 °C for 6 h.

Characterization

The phases were identified by means of X-ray diffraction (XRD) with a Rigaku D/max 2500 pc X-ray diffractometer with Cu Kα radiation (λ) 1.54156 (Å) at a scan rate of $0.04°s^{-1}$. The field emission scanning electron microscopy (FE-SEM) and the energy dispersive X-ray spectrum (EDS) were conducted on a Philips XL-30 field-emission scanning electron microscope operated at 20 kV, while the transmission electron microscopy (TEM) and high-resolution TEM (HRTEM) observations were carried out on a JEOL 2100F with an emission voltage of 200 kV.

Room-temperature hysteresis loops were collected on a VSM-7300 vibrating sample magnetometer (Lakeshore, USA).

Results

Figure 1a gives the typical XRD pattern of the as-prepared magnetite without the addition of CTAB, in which all the diffraction peaks can be indexed to a pure face-centered cubic phase ((fcc, space group Fd-3 m) (No. 227)) of magnetite. All the diffraction peaks in the XRD patterns can be indexed to face-centered cubic structure of magnetite according to JCPDS card no. 19-0629. The XRD result displays that single-phase spinel ferrite is

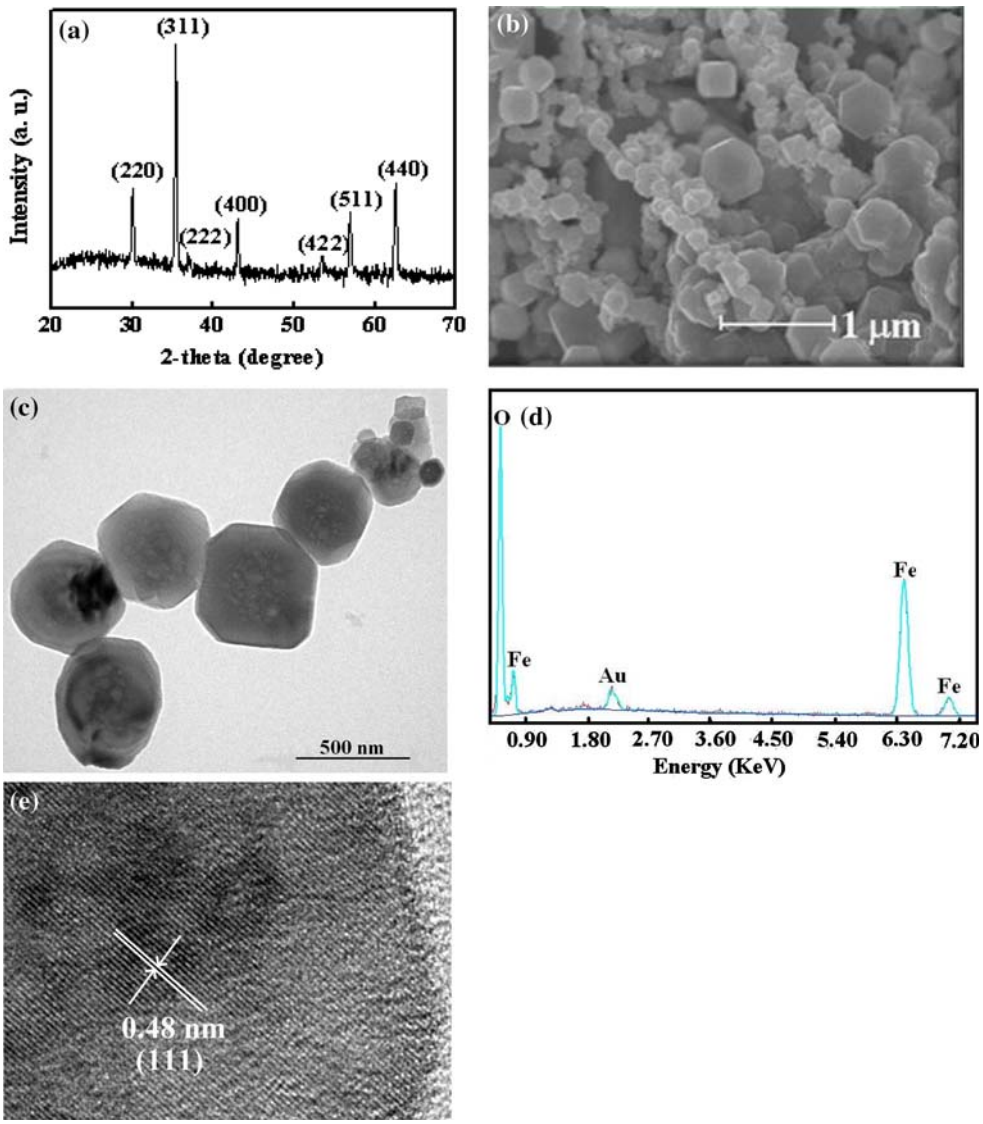

Fig. 1 As-prepared magnetite: **a** XRD pattern, **b** SEM photo, **c** TEM image, **d** EDS pattern, and **e** HRTEM image

synthesized by using the L-arginine and ferrous ions as raw materials. The sharpness of the X-ray diffraction peaks indicates that the Fe_3O_4 crystal is complete crystallization. Figure 1b shows that the sample is composed of little irregular particles with around 80 nm in diameter and 50-nm-thick hexagonal disks with about 200 nm in diameter. A typical TEM image of the Fe_3O_4 crystals is presented in Fig. 1c. Meanwhile, energy dispersive X-ray spectrum (EDS) (Fig. 1d) analysis confirms that the products consist only of Fe and O. The lattice fringes of the Fe_3O_4 crystals can be seen clearly from the High-resolution TEM (HRTEM), as shown in Fig. 1e, and the interplanar spacing was measured to be 4.8 Å, corresponding to the (111) planar spacing of cubic magnetite. Therefore, it is believed that the formation of magnetite during the hydrothermal process proceeds in a way with faster growth rate along ⟨001⟩ than along ⟨111⟩.

As far as we know, this study reports for the first time that L-arginine is used as precipitator to fabricate the single-phase Fe_3O_4 crystal. L-arginine is a ternary alkali (Fig. 2a) which possesses the strongest alkalinity among amino acids. By a series of contrastive experiments, we confirm that the pH values of this reaction system must be controlled in the range of 9–10 by adjusting the concentration of L-arginine for the preparation of pure magnetite. Additionally, the organic groups of L-arginine can adsorb on the surface of Fe_3O_4 crystals during the hydrothermal synthesis, which may make them possess high surface activity and have a potential application in biomedical field.

To shield light on the function of CTAB, we studied the samples obtained at different concentrations of CTAB during the hydrothermal synthesis using SEM, as shown in Fig. 2. We find that different concentrations of CTAB cause a dramatic change of the crystalline morphologies. When 0.02 mol L^{-1} of CTAB is introduced into the reaction system, dodecahedra are prepared (Fig. 2b). The edge lengths of the dodecahedra are 200 nm, and their thicknesses are about 80 nm. Increasing the concentration of CTAB to 0.06 mol L^{-1}, truncated octahedra with edge lengths about 200 nm together with little irregular particles were observed (Fig. 2c). Further increasing the concentration of CTAB to 0.1 mol L^{-1}, octahedra with truncated corners came out in the products as shown in Fig. 2d. From the above results, we can conclude that CTAB can induce the presence of new crystal planes. In addition, the presence of irregularly little particles in samples may be due to the quick growth rate in water solution. The formation of the hexagonal and polyhedral shapes can be expressed as a nucleation–crystallization growth mechanism.

Discussion

In a solution-phase synthesis, impurities or capping agents can change the order of free energies of different facets through their interaction with the crystal surfaces [17, 18]. As a result, the facet with a slower growth rate will be exposed more on the crystal surface [19]. Hence, it is very important to understand the crystal structure of the

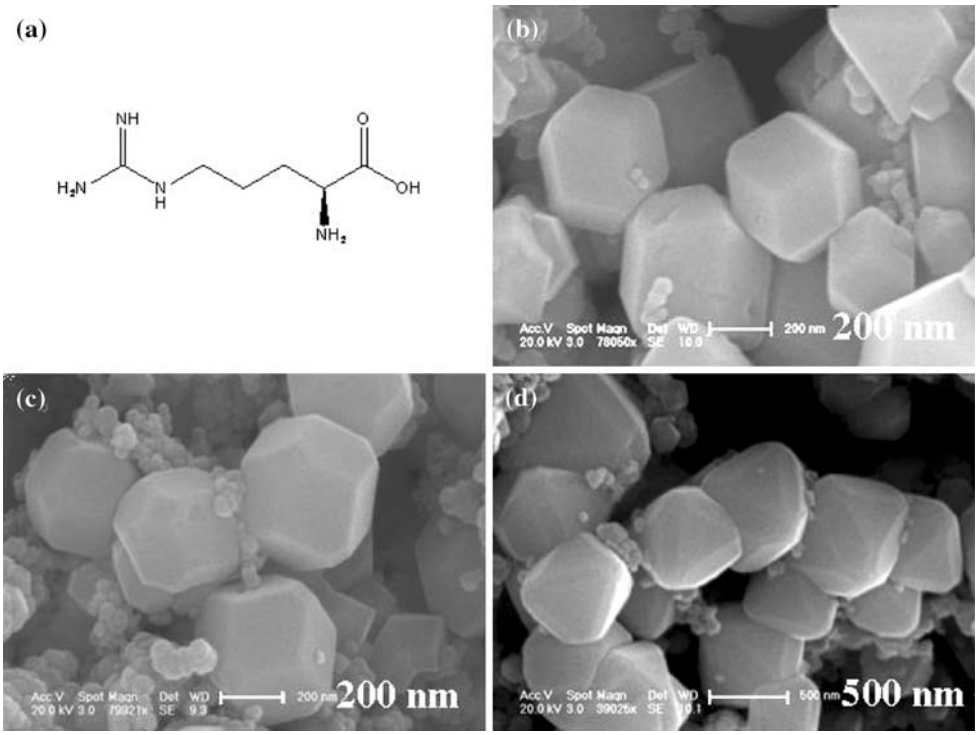

Fig. 2 **a** Configuration of L-arginine. SEM image of Fe_3O_4 ferrites obtained in different concentrations of CTAB: **b** 0.02, **c** 0.06, **d** 0.1 mol L^{-1}

magnetite. Figure 3 displays the schematic structure and crystal structure projections on the (111), (110), and (100) planes of the magnetite. Purple, red, and white balls in Fig. 3a indicate Fe at tetrahedral sites, Fe at octahedral sites, and O element. Purple and red balls in Fig. 3b, c, d denote Fe and O elements, respectively. In Fig. 3b, the repeating elemental sequence is $(O, Fe, O, Fe)_n$. The (111) faces contain Fe or O only. However, for the (100) and (110) planes, the O atoms are doubly coordinated by Fe atoms. Moreover, a (110) plane is shorter of singly coordinated ability than a (100) plane which can be observed from Fig. 3c, d. The crystals structure analysis shows that the magnetite adopts a face-centered cubic crystal structure and the general sequence for the surface energies of the magnetite structure was $\gamma\{111\} < \gamma\{100\} < \gamma\{110\}$ [20]. The external conditions of crystal growth directly affect the adoption of various crystal faces and the crystal relative surface free enthalpy. Thus, the external conditions influence the relative stability of the crystal surface, its growth rate, and the crystal morphology. It suggests that the driving forces such as the surface tension, the inherent crystal structure of the magnetite, and its chemical potential in the L-arginine solution may favor the anisotropic growth of the magnetite. From the point of view of the kinetics of crystal growth, if the crystal adsorbs the $-N(CH_3)_3$ groups on some areas of its surface, then the growth rate of the crystal in a certain direction will be confined. Therefore, the concentration of the CTAB can modify the growth kinetics of the growing crystal, which in turn leads to the anisotropic growth of the crystals. In addition, Swaminathan et al. pointed out that the ratio R, the growth rate along $\langle 100 \rangle$ to that along $\langle 111 \rangle$, plays a key role in determining the final morphology of the particles. With the increasing of R, the shape of the particles undergoes an evolution from a cube ($R = 0.53$) to a truncated octahedron ($R = 0.87$) and finally to an octahedron ($R = 1.73$). From the experimental results, we concluded that the concentration of the CTAB and the L-arginine solution were important in determining the R.

To clarify the transformations of the microstructural magnetite, the evolution processes are shown in Fig. 4. Since the morphology of the nanoparticles determines the fraction of (111) and (100) surfaces, it in turn will influence the effective surface anisotropy. The amino groups of L-arginine dissolve into NH_4^+ and OH^- in the water solution. The (111) planes possess higher surface energies at higher alkaline solutions without the addition of CTAB. The difference among the surface energies of the facets

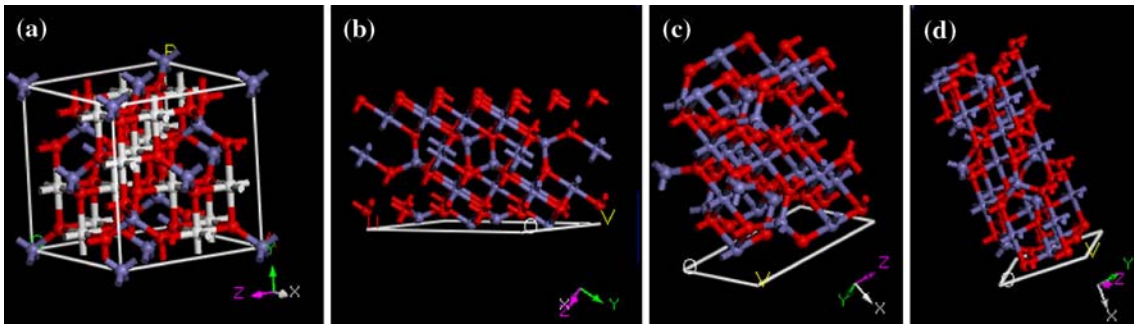

Fig. 3 **a** Schematic structure of magnetite. Crystal structure projection on the **b** (111) plane, **c** (110) plane, **d** (100) plane

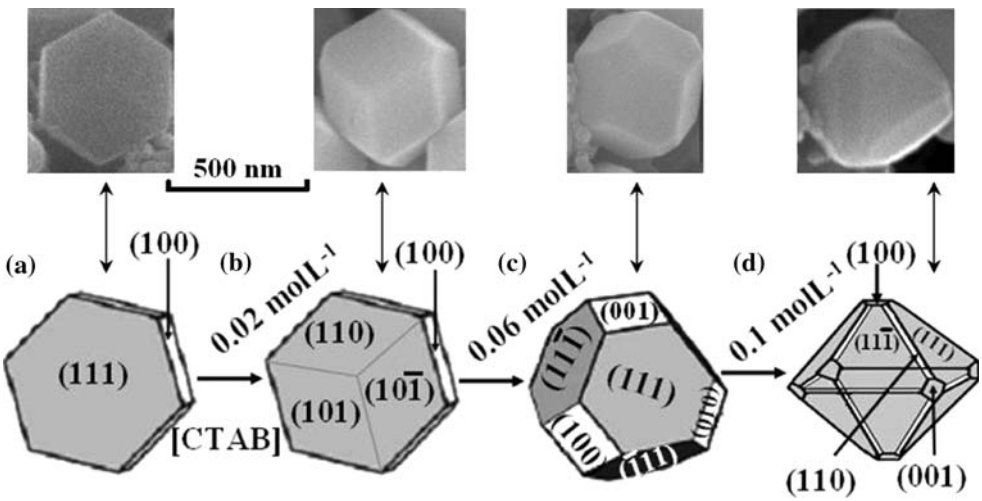

Fig. 4 Schematic illustration of the different crystal planes of polyhedra

reduced gradually for the adsorption effect. OH^- ions are selectively adsorbed on the (111) facets and enhance the crystal growth of (100) facets, and consequently the growth rate along the ⟨111⟩ direction is lower than that in the ⟨100⟩ direction, resulting in the formation of Fe_3O_4 disks. When different concentrations of CTAB were introduced into the hydrothermal reaction, the selective adsorption of $–N(CH_3)_3$ at different faces would change the growth rate of crystal planes. The competition for adsorption on (111) planes between the OH^- ions and $–N(CH_3)_3$ groups may decide the R value, that is to say the final morphologies of the magnetite. Moreover, the fractional adsorption of OH^- ions on the (100) facets and thus favor the formation of crystals with truncated corners.

Figure 5 shows the room-temperature hysteresis loops of Fe_3O_4 ferrite crystals synthesized with different concentrations of CTAB. The hysteresis loops almost reach saturation at 10000 Oe of applied field. From the measurements of magnetism, we can get the magnetic parameters, which are listed in Table 1. The highest M_s and the lowest H_c values among the Fe_3O_4 ferrite crystals are obtained without the addition of CTAB. However, the lowest M_s and the H_c values are obtained with the presence of 0.02 mol L^{-1} of CTAB. In summary, a higher M_s corresponds to a lower H_c for the Fe_3O_4 crystals. In this case, the magnetization mainly depends on the magnetic domain rotation, so the coercivity can be calculated by Stoner–Wohlfarth theory, $H_c = 2K/(\mu_0 M_s)$, where K is magnetocrystalline anisotropy constant and μ_0 is vacuum permeability. It shows that the H_c and the M_s are in reverse proportion, that is to say, a higher H_c leads to a lower M_s for the samples with cubic magnetocrystalline anisotropy. Shape anisotropy may be responsible for the different H_c values.

Table 1 Magnetic parameters obtained from hysteresis loops

[CTAB] (mol L^{-1})	0.00	0.02	0.06	0.10
M_s (emu/g)	93	76	84	80
H_c (Oe)	75	142	120	116

Conclusions

In conclusion, a simple and straightforward synthetic method has been developed for the preparation of multi-appearance magnetite. Hexagonal, dodecahedral, truncated octahedral, and polyhedral shapes can be obtained by changing the concentration of CTAB. L-arginine plays an important role in the formation of hexagonal shapes. The working together of L-arginine and CTAB may make for the preparation of polyhedra.

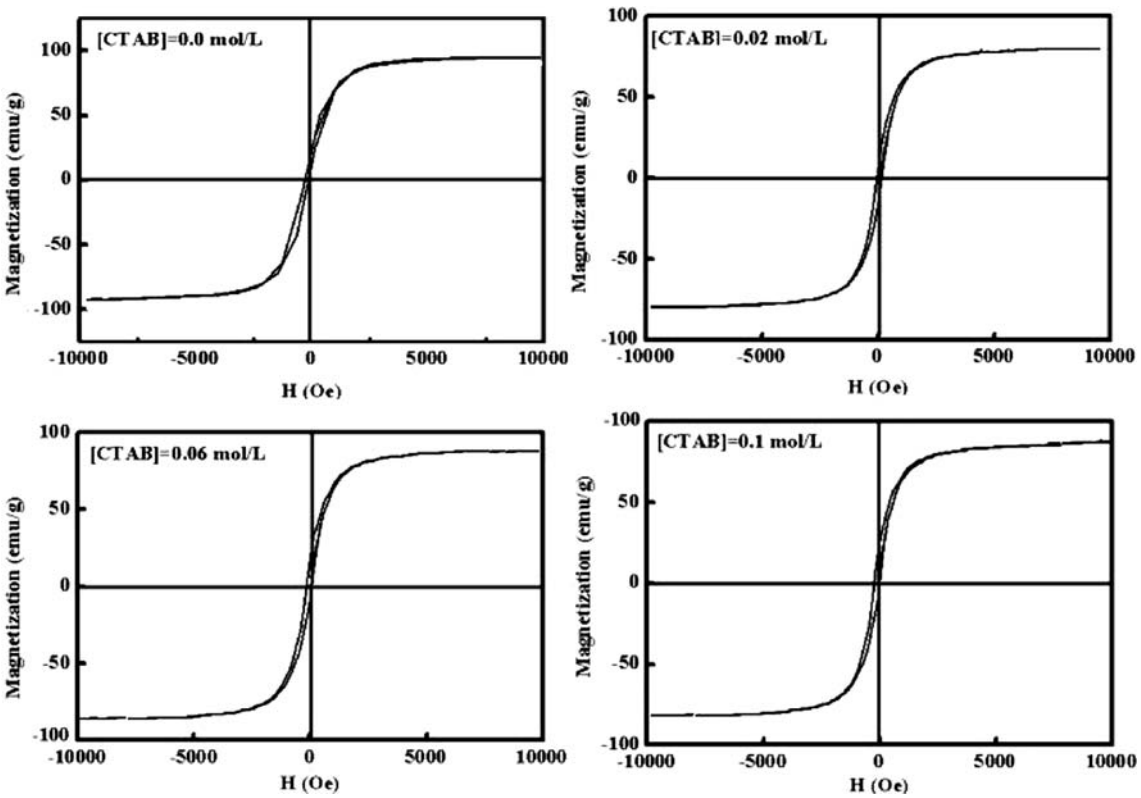

Fig. 5 Hysteresis loops of Fe_3O_4 ferrites synthesized with different concentrations of CTAB

Acknowledgements This study was supported by the Basic Research Expenses for the Special Funds of Jilin University.

References

1. Jiang J, Ai LH, Li LC (2009) J Mater Sci 44:1024. doi:10.1007/s10854-009-9885-4
2. Mohapatra S, Pramanik N, Mukherjee S, Ghosh SK, Pramanik P (2007) J Mater Sci 42:7566. doi:10.1007/s10853-007-1597-7
3. Puntes VF, Krishnan KM, Alivisatos AP (2001) Science 291:2115
4. Wang X, Zhuang J, Peng Q, Li YD (2005) Nature 437:121
5. Speliotis DE (1999) J Magn Magn Mater 193:29
6. Raj K, Mostowitz B, Casciari R (1995) J Magn Magn Mater 149:174
7. Oswald P, Clement O, Chambon C, Schuman-Claeys E, Frija G (1997) Magn Reson Imaging 15:1025
8. Berry C, Curtis ASG (2003) J Phys D Appl Phys 36:R182
9. Bourlinos AB, Bakandritsos A et al (2006) J Mater Sci 41:5250. doi:10.1007/s10853-006-0041-8
10. Liu XM, Fu SY, Zhu LP (2007) J Solid State Chem 180:461
11. Cho SB, Noh JS, Park SJ, Lim DY, Choi SH (2007) J Mater Sci 42:4877. doi:10.1007/s10853-006-0685-4
12. Liu XM, Fu SY, Xiao HM (2006) Mater Lett 60:2979
13. Liu Q, Huang HX, Lai LF, Sun JH, Shang TM, Zhou QF, Xu Z (2009) J Mater Sci 44:1187. doi:10.1007/s10853-009-3268-3
14. Zou GF, Xiong K, Jiang CL, Li H, Li TW, Du J, Qian YT (2005) J Phys Chem B 109:18356
15. Yu DB, Sun XQ, Zou JW, Wang ZR, Wang F, Tang K (2006) J Phys Chem B 110:21667
16. Chin KC, Poh CK, Chong GL, Van LH, Sow CH, Lin JY, Wee ATS (2007) J Phys Chem C 111:9136
17. Sun Y, Xia Y (2002) Science 298:2176–2179
18. Xiong Y, Xia Y (2007) Adv Mater 19:3385
19. Xiong Y, McLellan JM, Yin Y, Xia Y (2007) Angew Chem Int Ed 46:790
20. Swaminathan R, Willard MA, Mchenry ME (2006) Acta Mater 54:807